POAC'17
Busan, KOREA

Proceedings of the 24th International Conference on
Port and Ocean Engineering under Arctic Conditions
June 11-16, 2017, Busan, Korea

Preliminary 3D DEM Simulations on Ridge Keel Resistance on Ships

Hanyang Gong[1], Arttu Polojärvi[1], Jukka Tuhkuri[1]
[1] Aalto University, School of Engineering, Department of Mechanical Engineering, P.O. Box 14300, FI-00076 Aalto, Finland

ABSTRACT

Ice ridge resistance of ships operating on Arctic seas is of importance when estimating the ship traffic emissions and the efficiency of ship transport systems. Here we use 3D discrete element method (DEM) to simulate the interaction between a ridge keel and a ship. In this preliminary study, we will present results from simulations with various ridge keel lengths and accounting for the symmetry of the interaction scenario. We also study the effect of ridge keel widths on the keel resistance in our simulations.

KEY WORDS: Ice ridge; Keel resistance; Ship; Keel width; 3D DEM.

INSTRUCTION

Ice ridge resistance on ships has a central role in route planning and optimization of marine transport on Arctic seas. Ridge resistance is usually divided into components related to the structure of a ridge: keel (underwater pile of loose or partly cohesive ice rubble), consolidated layer (refrozen layer close to water line), and sail (rubble pile above water line). In recent transit models (Ehle, 2012; Kuuliala et al., 2016), the consolidated layer resistance is assumed equal to that of level ice (Riska, 2014), while the keel, or ice rubble, resistance is derived based on the methods presented by Mellor (1980) and Malmberg (1983). (Sail is small in volume and often neglected.) This paper focuses on three-dimensional discrete element method (DEM) study on rubble resistance, and on the effect of rubble pile geometry on the resistance.

The only analytical methods for estimating the keel resistance were developed by Keinonen (1979) and Malmberg (1983). They assumed that the rubble in the keel behaves like a body of homogeneous and isotropic granular material, which has a semi-infinite boundary, and applied Coulomb failure criterion together with Rankine theory on its failure. Many analytical approaches on the ridge-structure interaction follow similar ideas (Dolgopolov, 1975; Cammaert et al., 1993; Croasdale, 2012; Palmer and Croasdale, 2013). Modelling of the ice rubble has been performed using continuum models (Heinonen, 2004; Serre, 2011 a, b) and discrete approaches that account for the individual ice blocks in the rubble (Hopkins, 1992; Hopkins, 1998; Hopkins and Hibler, 1991; Polojärvi and Tuhkuri, 2009, 2012; Polojärvi et al., 2012). Liu et al. (2016) recently used dilated polyhedron-based DEM to study

ice floe-ship hull interaction. DEM enables studies on the rubble resistance without choosing a rubble material model and making a priori decision on rubble pile failure criterion.

The main finding of this paper is that the rubble pile width has a strong effect on the resistance. This effect is not accounted for in the analytical models. We will first introduce the simulation set-up. Then the keel resistance records are presented and assumptions used in the modelling are addressed. After this, the results on the effect of rubble pile width on the resistance are presented. Before concluding our paper, we compare the simulation-based resistance values to those measured in the field and given by the analytical formulas.

SIMULATION SET UP

The 3D DEM code we use is an in-house code of Aalto University Ice Mechanics Group (Polojärvi and Tuhkuri, 2009, 2012). In brief, the simulations are explicit and we model the ship and all the blocks in the rubble as polyhedral rigid bodies. The ship-to-block and block-to-block contacts cause forces, which compose of a normal component due to elastic and viscous damping forces, and a tangential component due to friction. In addition to contact forces, buoyant, gravitational and drag forces act on the blocks. The block sizes vary randomly with a distribution given by Kulyakhtin (2014). The geometry of the modelled ship is that of M/T Uikku. All simulation parameters are given in Table 1.

The simulation basin is illustrated by Figure 1. The whole basin was covered by a rigid plate mimicking the ice cover on top of the ice rubble. The basin extended far enough into the x- and z-directions to keep any of the blocks, or the ship, from interacting with the basin walls in these directions. As will be explained below, the basin extent into the y-direction was varied, as in this direction the basin walls were in contact with the rubble pile. The centerline of the ship was parallel to the x-axis and aligned with the centerline of the basin. The model has a plane of symmetry on xz-plane and we could use a half model in our simulations (rigid wall at $y = 0$ and rubble in the half domain $y < 0$ only).

We tested a number of pile widths (into the x-direction) and lengths (into the y-direction), and ran simulations with two different ice-ice friction coefficient μ_i values as summarized in Table 2. Figures 2a and b describe the pile geometries used. The narrowest of the modelled piles had a triangular shape (Figure 2a) while the shape of the wider keels was trapezoidal (Figure 2b). All piles had a depth h of 5 m and pile angle of repose of 30° (Timco and Burden, 1997). We also justified the use of the half model by running simulations with full and half models. Naturally, the resistance of a full rubble pile model having the length l_f should be the double of that yielded by a corresponding half model with length $l_h = 0.5 l_f$.

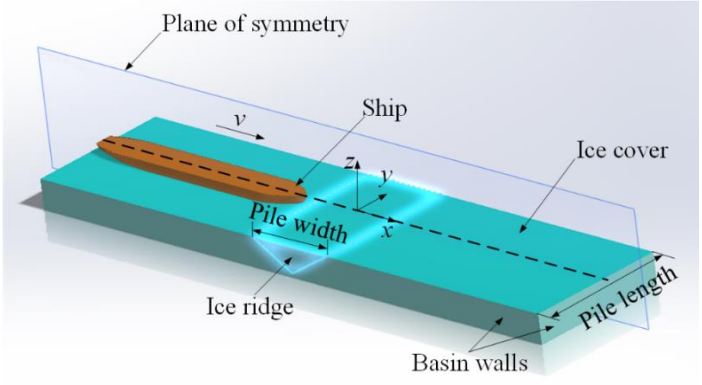

Figure 1. A sketch of the simulation basin and the coordinate system used in this paper.

Table 1. The main parameters used in simulations. The geometry of the modelled ship was that of M/T Uikku. Figure 2 illustrates the pile dimensions given in the Table.

	Parameter	Unit	Value
General	Gravitational acceleration	ms^{-2}	9.81
Contact	Penalty term	-	$1 \cdot 10^{7}$
	Damping constant	-	$5 \cdot 10^{5}$
	Time step	s	$5 \cdot 10^{-5}$
Ice blocks	Thickness	ms^{-2}	0.3
	Block aspect ratio	-	0.6…15
	Ice-ice friction coefficient μ_i	-	0.3, 0.6
	Mass density	kgm^{-3}	920
Water	Mass density	kgm^{-3}	1010
Rubble piles*	Pile depth h	m	5
	Pile angle θ	°	30
	Pile width w	m	17.3…80
	Pile length l_f (= $2l_h$)	m	60…100
Ship	Waterline length	m	150
	Parallel midbody L_m	m	67.5
	Breadth B	m	22.2
	Draft T	m	9.5
	Waterline half-angle α	°	25.2
	Stem angle φ	°	29.7
	Ship-ice friction coefficient μ_s	-	0.1
	Ship velocity v_{ship}	ms^{-1}	1

*all values refer to the initial pile geometry. Indices f and h respectively refer to full and half model.

Table 2. Summary of the simulations used in this paper. All of these simulations were ran with ice-ice friction coefficient μ_i values 0.3 and 0.6, so that the total number of simulations was 20. Figure 2 illustrates the pile dimensions given in the Table.

	Pile length* l_f	Pile length* l_h	Pile width w
Full model	100	-	17.3
	80	-	17.3
	60	-	17.3
Half model	-	50	17.3
	-	40	17.3
	-	30	17.3
	-	30	30
	-	30	40
	-	30	60
	-	30	80

*all values refer to the initial pile geometry. Indices f and h respectively refer to full and half model.

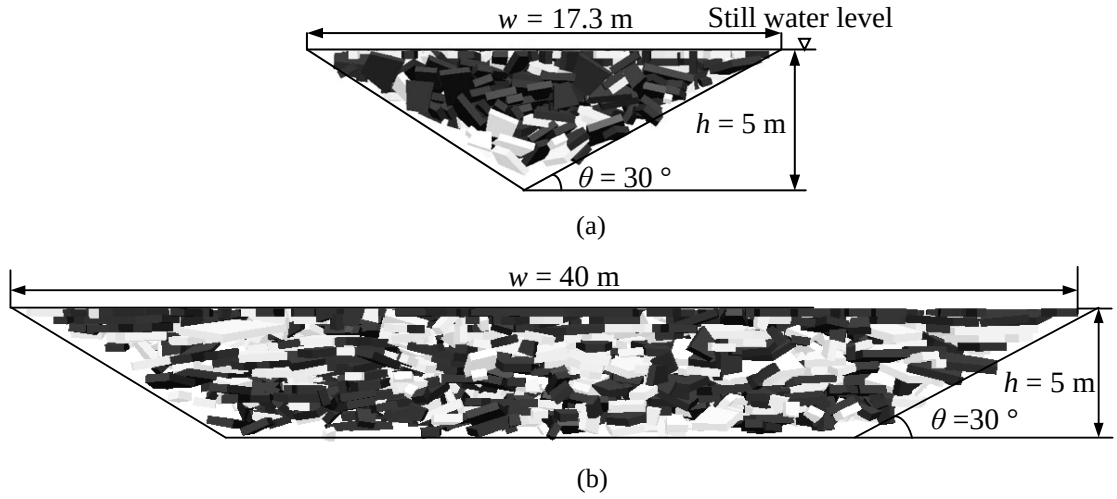

Figure 2. The pile geometries used in our simulations: (a) is the narrowest modelled pile with a triangle shape and (b) has a trapezoidal shape for the wider pile.

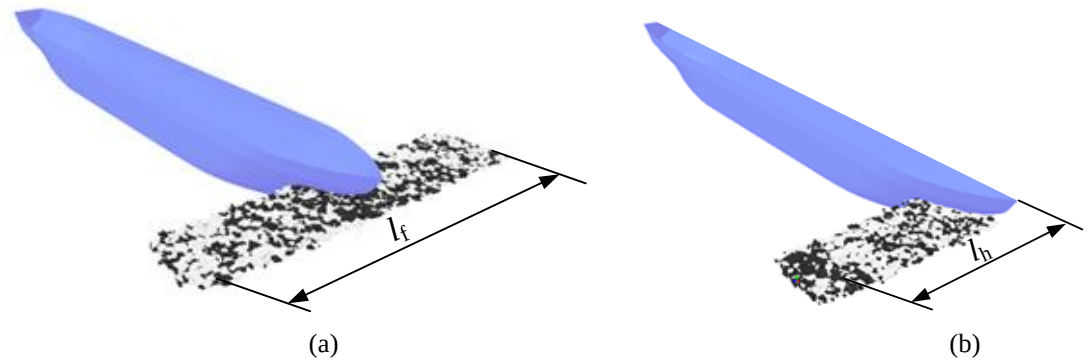

Figure 3. Simulation snapshots of the actual ship-rubble interaction: (a) to illustrate the ship penetration through the full model with rubble pile length of l_f and the half model with l_h (b).

The simulations were performed in two stages: first the ice rubble pile was generated and then the ship was driven through the rubble. The ice rubble was generated by releasing ice blocks underwater, and by letting the simulation run until the viscous damping and frictional forces had dissipated virtually all of the kinetic energy of the system (Polojärvi and Tuhkuri, 2009). The basin cover on the top of the rubble provided frictional resistance on the rubble pile so that it would not dissolve. After the rubble mass had become to rest, the blocks that did not belong to the wanted pile geometry were removed from the simulation.

Figures 3a and b show two snapshots from a simulation of the actual ship-rubble interaction. In these simulations, the ship moved with a constant velocity v_{ship} into the positive x-direction and penetrated the rubble pile. The basin cover did not interact with the ship (no contact forces between the ship and the cover) nor did the cover fracture. Hence, the cover provided just frictional resistance for the rubble pile. On each time step, all of the ship-block contact forces were superposed into a force resultant $\mathbf{f}_S = [f_{sx} \quad f_{sy} \quad f_{sz}]^T$ acting on the ship. The rubble resistance was defined as $R = -f_{sx}$.

RESULTS

The Keel Resistance Records

Figure 4 shows ridge keel resistance - ship penetration (R-δ) records from two simulations: one with a full model (l_f = 60 m), and another with a half model (l_h = 30 m). The pile width w and the ice-ice friction coefficient μ_i were 17.3 m and 0.3, respectively, and the half model resistance data is multiplied by a factor of two. The noise in the force record is due to the individual ice blocks within the rubble, which had a random initial configuration, impacting the ship hull. While the initial configuration of the rubble affected this noise, the general features of the R-δ records were similar for all configurations.

Figure 4 describes the main features of the R-δ records. R initially increases up to a peak value R^p, which is reached when the ship bow has nearly penetrated the whole ridge. Subsequently, R decreases and reaches an approximately constant value for a period, during which only the midbody of the ship interacts with the rubble. During this period, R is due to the frictional forces acting on the midbody of the ship. (With large w, R did not show this period of a constant value, as seen below.) When the whole ship has passed through the rubble, R decreases to zero. The change in ice-ice friction coefficient μ_i did not affect the main features of the R-δ records, but only increased the R throughout the interaction process.

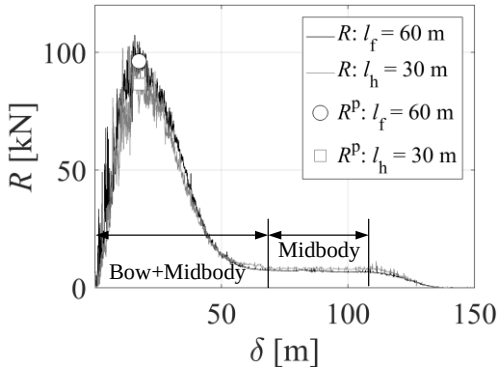

Figure 4. The resistance (R) - ship penetration (δ) records for a full model (l_f = 60 m) and a half model (l_h = 30 m). The peak resistance R^p is indicated with a marker. The rubble width w = 17.3 m and the ice-ice friction coefficient μ_i = 0.3. Half model R is multiplied by two.

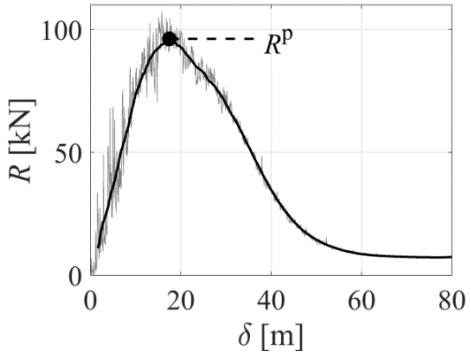

Figure 5. The resistance-penetration record (gray), the running average of it (black) and the peak resistance R^p. The data is from a simulation with full model, window size for running average 6 m, pile length l_f = 60 m, pile width w = 17.3 m, and ice-ice friction coefficient μ_i = 0.3.

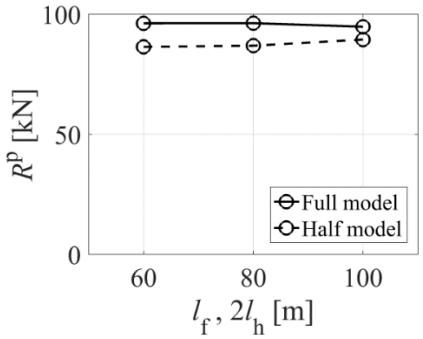

Figure 6. Peak resistance R^p from simulations with the full models and the half models. R^p is plotted as a function of pile length. Half model R^p values are multiplied by a factor of two.

Figure 4 further indicates the peak resistance R^p values of the simulations with two markers. The R^p values were defined as illustrated in Figure 5: R^p was the maximum of the running average on the R-δ data. The running average enabled us to study the general trends in R^p data as it filtered out the configuration-depended noise in the R-δ records. The window size for the running average was 6 m. As Figure 5 shows, the general features of the R-δ records are well preserved when the running average with this window size is used.

Figure 6 compares the R^p values from the simulations with the full model to those with the half model. The data is from simulations where the pile width w and the ice-ice friction coefficient μ_i were 17.3 m and 0.3, respectively. The R^p values are plotted against pile length l, and it can be seen that the pile length has virtually no effect on the R^p values. The figure also shows that the R^p values in the simulations with the full model are 6-10 % higher than in the simulations with the half model. Based on this, and the data in Figure 4, we use the half model with pile length l_h = 30 m in the further studies.

The Effect of Keel Width on the Resistance

Figure 7 presents the R-δ records from five simulations that had different pile widths w (see Table 2 for the simulation matrix). It is interesting that w has a strong effect on the R-δ record: as w increases, so does the peak resistance value R^p. Further, the peak resistance value R^p is reached later in wider rubble piles.

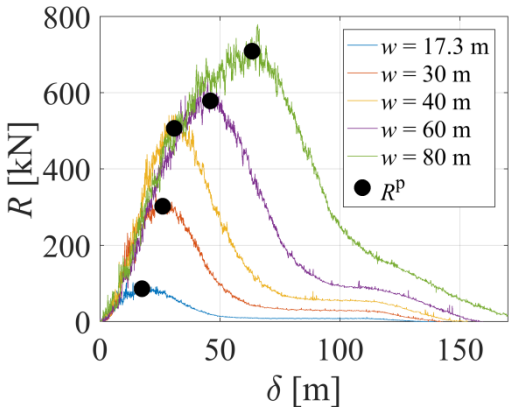

Figure 7. The keel resistance-ship penetration records from simulations with different pile widths w. The figure also indicates the peak resistance R^p values. In these simulations, a half model with l_h = 30 m and μ_i = 0.3 is used. All values are multiplied by a factor of two.

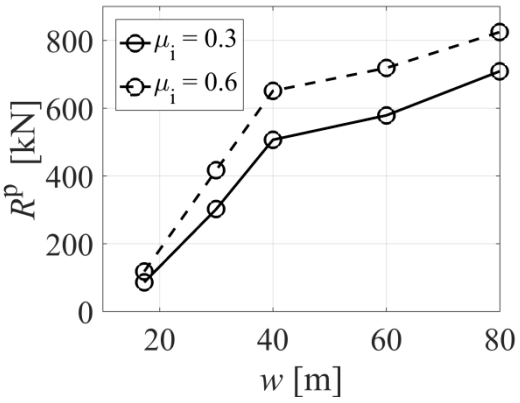

Figure 8. The peak resistance-pile width (R^p-w) records from simulations for two ice-ice friction coefficients μ_i. All values are multiplied by a factor of two.

Additionally, for w < 60 m, the R value for the interval of constant resistance increases with w (see also Figure 4). This is another manifestation that this interval of constant R is due to the frictional resistance acting on the midbody of the ship: the total contact area between the midbody and the rubble mass increases with w. Further, the interval of constant R starts later during the interaction process as w is increased. However, once w is large enough (80 m), the stern of the ship enters the rubble before the interval of constant R would start, and no period of constant R occurs.

The values for peak resistance R^p are plotted against w and μ_i in Figure 8. The effect w on R^p is drastic. R^p shows an eight-fold increase with the w values used (17.32 … 80 m). The R^p-w data show two distinct regimes. When w < 40 m, R^p shows a strong dependency on w, whereas when w > 40 m, the increase in R^p is slower. Ice-ice friction coefficient μ_i has a clear, but less pronounced effect on R^p values. Increasing μ_i from 0.3 to 0.6 increased R^p by 16-38 %, depending on w. The effect of μ_i was strongest with low w and then got weaker as w increased. The study on the reasons behind these results is out of the scope of this paper.

DISCUSSION

We compared the simulation results to field data and analytical formulas. The field-measured ridge resistance of a ship having close to same dimensions as the one modelled here was about 1900 kN for a ridge with a depth of 5 m (Keinonen, 1979). This is much higher than the peak keel resistance R^p yielded by our simulations. We are looking into this discrepancy, but unfortunately, there is a lack of a detailed description on the geometry (especially its width), and even on the existence of a potential consolidated layer of the full-scale ridge.

We also compared the results to the analytical formula for rubble resistance R_A by Malmberg (1983), which is recommended by a report for Finnish-Swedish ice class rules (Riska, 1997). The formula reads (Table 1 describes most of symbols)

$$R_A = C_1 T h \left(\frac{B}{2} + h \tan\psi \cos\alpha \right) (\mu_s \cos\alpha + \sin\psi \sin\alpha) + C_2 T L_m \left[K_0 h + \left(\frac{h}{T} - \frac{1}{2} \right) B \right], \qquad (1)$$

where L_m is the length the part of the midbody that is parallel to the centerline of the ship and the term h/T-1/2 should always be positive or it is to be set to zero. The angle ψ is the normal angle from horizontal at the bow, and is obtained from ψ = arctan(tan φ / sin α), where φ and α are the stem angle and waterline half-angle of the ship, respectively. Further, K_0 is the

coefficient of active pressure at rest, which describes the pressure due to the static ice rubble on the ship, and should be 0.27 according to (Riska, 1997). The constants C_1 and C_2 are

$$C_1 = (1-p)(\rho_w - \rho_i)gK_p \quad \text{and} \quad C_2 = (1-p)(\rho_w - \rho_i)g\mu_s, \tag{2}$$

where p is the rubble porosity, μ_s is the ship-ice friction coefficient and g is the gravitational acceleration. Further, $K_p = \tan^2(45+\phi/2)$ is the coefficient of passive pressure, where ϕ is the internal friction angle of the rubble pile.

With the dimensions and parameters of our simulations, the resistance R_A given by Equation 1 is about 1000 kN, when we set ϕ = 40° and p = 0.3. These are typical ϕ and p values assumed for ice rubble (Kulyathkin, 2015). (Porosity p in our simulations was about 0.3 (Polojärvi and Tuhkuri, 2009) but we have not tested the simulated rubble for ϕ.) Peak resistance R^p in our simulations with the keel width w = 80 m was about 700-800 kN depending on μ_i (see Figure 8). The peak resistance values for wide rubble piles in our simulations compare well with R_A values given by Equation 1 when we use ϕ and p values typical for natural ice rubble.

The R^p values however vary with w as Figure 8 showed. We believe that this is the first time the dependency of R on w is discussed, and that this is a finding of potential importance. Route planning and optimization for Arctic transit often rely on estimates on ridge resistance. The often-used analytical methods (Keinonen, 1979; Mamlberg, 1983; Riska, 1997) for ridge resistance do not account for the effect of w. They assume that the pile width is infinite, and effectively then, apply to rubble fields rather than individual ridge keels. In other words, it is possible, that the resistance for ridge keels having limited w is often overestimated (or, at least, that the contribution of the ice rubble on ridge resistance is overestimated).

CONCLUSIONS

We simulated ship-ice rubble interaction process using 3D DEM. In these simulations, a ship penetrated through a non-cohesive rubble pile of width w with a constant velocity. As a result, rubble resistance R curves were achieved. Our main finding was that the R depends on w. This finding may have implications on, for example, marine traffic route optimization and transit simulations.

ACKNOWLEDGEMENTS

We are grateful for the support from the Academy of Finland through the project Kara-Arctic Monitoring and Operation Planning Platform (KAMON).

REFERENCES

Croasdale, K. R., 2012. A simple model for first-year ridge loads on sloping structures. In: *Proc. of the Int. Conf. and Exhibition on Performance of Ships and Structures in Ice*.

Dolgopolov, Y., Afanasiev, V. P., Koren'Kov, V. A., & Panfilov, D. F., 1975. Effect of hummocked ice on the piers of marine hydraulic structures. In: *International Symposium on Ice Problems, 3rd, Proceedings*, pp.460-477.

Ehle, D., 2012. Ships Breaking through Sea Ice Ridges. In: *Proceedings of the Twenty-second International Offshore and Polar Engineering Conference*, pp.1188-1193.

Heinonen, J., 2004. *Constitutive modeling of ice rubble in first-year ridge keel*. Doctoral thesis. Helsinki University of Technology. VTT Publications 1235-0621 536. VTT Technical Research Centre of Finland, Espoo, Finland.

Riska, K., Wilhelmson, M. & Englund, K. and Leiviskä, T., 1997. *Performance of Merchant Vessels in Ice in the Baltic*. Finnish Maritime Administration, Winter Navigation Research Board, Rpt. No. 52, Helsinki, 73 p.

Hopkins, M.A., Hibler, W.D. and Flato, G.M., 1991. On the numerical simulation of the sea ice ridging process. *Journal of Geophysical Research: Oceans*, 96(C3), pp. 4809-4820.

Hopkins, M. A., 1992. *Numerical simulation of systems of multitudinous polygonal blocks*. Technical Report 92-22, Cold Regions Research and Engineering Laboratory, CRREL. 69 p.

Hopkins, M.A., 1998. Four stages of pressure ridging. *Journal of Geophysical Research: Oceans*, 103(C10), pp.21883-21891.

Keinonen, A., 1979. *An analytical method for calculating the pure ridge resistance encountered by ships in first year ice ridges*. Doctoral thesis. Helsinki University of Technology.

Kulyakhtin, S. and Høyland, K.V., 2014. Study of the Volumetric Behaviour of Ice Rubble Based on Bi-Axial Compression Data. In: *22nd IAHR Int. Symposium on Ice*, pp.235-240.

Kulyakhtin, S. and Høyland, K.V., 2015. Ice rubble frictional resistance by critical state theories. *Cold Regions Science and Technology*, 119, pp.145-150.

Kuuliala, L., Kujala, P., Suominen, M. and Montewka, J., 2016. Estimating operability of ships in ridged ice fields. *Cold Regions Science and Technology*, 135, pp.51-61.

Liu L., Sun S., Ji S., 2016. Dilated Polyhedra-based Discrete Element Simulation of Ice Loads on Ship Hull. In: *23rd IAHR International Symposium on Ice*, pp.1-8.

Malmberg, S., 1983. *Om fartygs fastkilning i is*. Master's thesis. Helsinki University of Technology.

Mellor, M., 1980. Ship resistance in thick brash ice. *Cold Regions Science and Technology*, 3(4), pp.305-321.

Palmer, A. and Croasdale, K., 2013. *Arctic offshore engineering*. World Scientific: Singapore.

Polojärvi, A. and Tuhkuri, J., 2009. 3D discrete numerical modelling of ridge keel punch through tests. *Cold Regions Science and Technology*, 56(1), pp.18-29.

Polojärvi, A., and Tuhkuri, J., 2012. Velocity effects in laboratory scale punch through experiments. *Cold Regions Science and Technology*, 70, pp.81-93.

Polojärvi, A., Tuhkuri, J. and Korkalo, O., 2012. Comparison and analysis of experimental and virtual laboratory scale punch through tests. *Cold Regions Science and Technology*, 81, pp.11-25.

Timco, G.W. and Burden, R.P., 1997. An analysis of the shapes of sea ice ridges. *Cold regions science and technology*, 25(1), pp.65-77.

Serré, N., 2011a. Mechanical properties of model ice ridge keels. *Cold Regions Science and Technology*, 67(3), pp.89-106.

Serré, N., 2011b. Numerical modelling of ice ridge keel action on subsea structures. *Cold Regions Science and Technology*, 67(3), pp.107-119.